32 chapter

Food Microstructure Techniques

Jinping Dong (✉) • Var L. St. Jeor
Research and Development,
Cargill, Inc.,
14800 28th Ave. N, Plymouth, MN 55447, USA
e-mail: Jinping_Dong@cargill.com; Var_StJeor@cargill.com

S. Nielsen (ed.), *Food Analysis*, Food Science Text Series,
DOI 10.1007/978-3-319-45776-5_32,

32.1 INTRODUCTION

While the main function of food is to provide enjoyment (e.g., flavor, aroma, texture) and nutrition (including energy), some other functionalities (e.g., desired shelf life, improved health benefit, friendly labeling) are also necessary for consumer appeal. One of the trends in food research is to be able to design and produce the food with any desired functionality. To achieve this, many approaches are being taken by different researchers and food manufacturers, with one prevailing approach being to understand and control food structures, especially at the microscopic scale. The study of food microstructures typically involves three aspects – visualization, identification, and quantification – with each requiring the aid of different tools.

Food is a complex and often heterogeneous system. Both fresh (typically dominated with cellular structure) and processed (microscopic domains formed by mixed ingredients) foods contain structures that cannot be directly seen with naked eyes. Human eyes are capable of seeing things down to about 1 μm with proper lighting (compared to ~20 to 50 μm being the diameter of a human hair). Many biological cells are a few micrometers in size, but they are not usually visible to our eyes because good illumination is not always available. They appear big and clear under a regular light microscope. Some good salad dressing emulsions have oil or water droplets well below 1 μm in diameter. Elemental plant fibers have a diameter of only a few nanometers. All these require a higher resolving power microscope such as a scanning electron microscope (SEM).

Determining the morphology of the food with the help of microscopes is only one part of the microstructure elucidation. Identifying the distribution of ingredients with different chemical and physical characteristics gives another insight, and this often requires a chemical imaging tool [e.g., Fourier transform infrared (FTIR), Raman, fluorescence, or confocal laser scanning microscope] or a physical structural tool for understanding molecular arrangement or crystallinity (e.g., x-ray diffractometer).

Modern microscopy and chemical imaging tools allow users to not only determine food morphology and ingredient distribution but also to quantify dimension parameters, concentrations, fractions, and kinetic constants. Using x-ray computed tomography, quantification can be done in 3-D with nondestructive imaging. Microscale interactions and forces also can be probed among the food ingredients with the help of instruments such as atomic force microscope. Values obtained from quantitative measurements are the last piece of the puzzle to solve food microstructures.

All of the microstructure techniques listed above will be briefly introduced in this chapter. Many of them were not initially invented for food applications but have been borrowed by food researchers to understand food and to correlate structure to its functionality. This chapter is not intended to be comprehensive in either breadth or depth regarding these techniques but rather to provide an overview, with references for more details. Note that the chapter will not cover measuring particle size and shape (see Chap. 5, Sect. 5.5.2.3) or color (see Chap. 31) and will refer to a number of spectroscopy chapters (Chaps. 7 and 10) as they relate to techniques for characterizing food microstructure. Because there are so many acronyms associated with instrumentation to evaluate food microstructure, a listing of acronyms used in this chapter is given.

32.2 MICROSCOPY

32.2.1 Introduction

One of the most frequently used family of instrumental techniques for analyzing foods and food microstructures is **imaging**. Imaging has traditionally been referred to as microscopy, but microscopy is quickly becoming only one aspect of the much larger field now being identified as imaging. **Microscopy** is the art and science of using microscopes as scientific investigative tools. Since the original development of light microscopes [1, 2], drastic improvements have been achieved in our ability to see in magnification and to differentiate in feature contrast. Example imaging agents include light (photons), x-rays (high-energy photons), electrons, ultrasound, microwaves, radio waves, etc. Most of the imaging agents are based in, and are a part of, the electromagnetic spectrum. Each of these techniques is subdivided into various imaging methods.

Microscopes were invented to visualize objects that cannot be seen by human eyes. How small of an object that can be clearly identified with the microscope determines the resolving power of the instrument. **Resolution** is the ability to distinguish or resolve two small points, which are very close together, as two separate entities. Factors that affect a microscope's resolution include the properties of the imaging agent (e.g., wavelength of the light) and the focusing power of the instrument (e.g., numerical aperture of the objective for light microscope). These are taken into account with a simple equation to calculate the **theoretical resolution limit** for a given microscope's primary or objective lens:

$$R = \lambda / 2NA \tag{32.1}$$

where:

R = resolution (theoretical resolution limit, minimum distance of the two adjacent objects)
λ = wavelength of the visualizing agent
NA = numerical aperture of the lens [proportional to the refractive index and sin (θ), where θ is the half angle of the incidence of the incoming light to the lens]

Inherent to any lens are imperfections, referred to as **aberrations**, which can cause images to appear distorted, out of focus, with colored fringes, etc. Correction of optical aberrations includes improvement of lens fabrication and grinding techniques, optimization of glass formulations, application of antireflection coatings, control of optical pathways, and combination of multiple lens elements.

Misalignment of the optical illumination is another factor that impacts a lens' optimum resolving power. Specific procedures and the care from the microscopist are needed to achieve perfect alignment and focus of the light beam to give uniform and bright illumination of the specimen. The alignment procedure is called **Köhler alignment**, named after August Köhler, a German physicist and microscopist [3].

32.2.2 Light Microscopy

32.2.2.1 *Introduction*

Light microscopy, as referred to in its name, employs light (or photons) as the imaging agent and magnifying lenses to visualize objects that cannot be seen with naked eyes. Light can be either reflected off of or transmitted through the sample and is then directed through the objective lens to the eye piece(s). Depending on the instrument design, there are two major categories of LMs, namely, stereo and compound microscopes. **Stereo** is a word related to **parallax**, or the difference between the angle of light arriving at your two eyes. These differing angles of view allow the brain to interpret the two differing views [each a two-dimensional (2-D) image] as though one is seeing a single three-dimensional (3-D) image. Stereo microscope typically has low magnification (2–100×) but has long working distance and large viewing depth, which make it easy for visualizing large and odd-shaped specimen. **Compound** references the compound nature of multiple lenses working together to achieve a clear, in focus, magnified image. It usually works in higher magnification range (40−1200×), with the combination of the lenses from objectives and eyepieces.

32.2.2.2 *Contrasting Modes*

In LM there are many ways to manipulate the light both before it reaches the specimen and after it interacts with the specimen to highlight certain features. Many of these are commonly used in the food industry and constitute what are called **contrasting** or **imaging modes** of light microscopy. A partial list of imaging modes includes bright-field, dark-field, phase contrast, birefringence (or cross polarization), differential interference contrast (DIC), and oblique lighting. With the exception of bright-field mode (the simplest lighting mode), each of these alternant modes requires additional special fixtures to be attached to the microscope to accomplish the desired effect. When in use, they often need to be aligned so they interact with the light correctly. What the various imaging modes produce in image can be referred to as special effects. They do not usually increase resolution per sé, but they can allow one to distinguish structures that may not be easily evident using other imaging modes. Starch is a classic example of a food component that can be examined using any of the imaging modes listed (Fig. 32.1).

32.2.2.3 *Fluorescence Microscopy*

Fluorescence is the light emitted from an atom, a molecule, or a material excited to the electronically active state (see Chap. 7, Sect. 7.3). The wavelength or energy of the excitation light is characteristic to the chemical bonds within a molecular or to the chemical/physical state of a material. By applying proper light sources and optical filters, fluorescence can be used to give unique contrast in light microscopy. Optical filters are added to a bright light source to select target wavelength for excitation, or **excitation spectrum**, and fluorescence filters are added after the sample to capture **emission spectrum**. Fluorescent stains, which contain functional groups that fluoresce upon excitation (called fluorochrome), also can be added to a sample to contrast components that they have strong affinity with. Staining can be done positively (e.g., staining the target structure) or negatively (e.g., staining nontarget structures). Many food materials contain natural fluorochrome. When a proper excitation wavelength is selected, bright color from fluorescence emission can be easily visualized under the light microscope. Figure 32.2 shows the aleurone layer within a wheat kernel that auto-fluoresces bright blue, making that particular layer of cells become obvious to the viewer, over any other cell types within the wheat kernel.

32.2.2.4 *Histology*

Histology, which refers to sample staining combined with light microscopy [4], is often used in biology and medicine to study cells and tissues. Samples are typically sectioned in some ways to create relatively thin slices with even thickness of the materials. This procedure is known as **microtomy** and usually involves a microtome or other mechanical cutting tools [5]. Histology has been applied in food research for a long time owing to its unique contrasting capability. The numerous stains available on the market [6–8] are each designed to stain different things different colors. Stains interact with food ingredients mostly through physical interactions, which make the affiliated ingredients appear with the color of the stain itself. However, the stain-ingredient interaction sometimes can shift the color spectrum. For example, although common cornstarch stains blue with iodine, waxy cornstarch stains red (Fig. 32.3). This is the result of amylopectin dominating the starch in the waxy

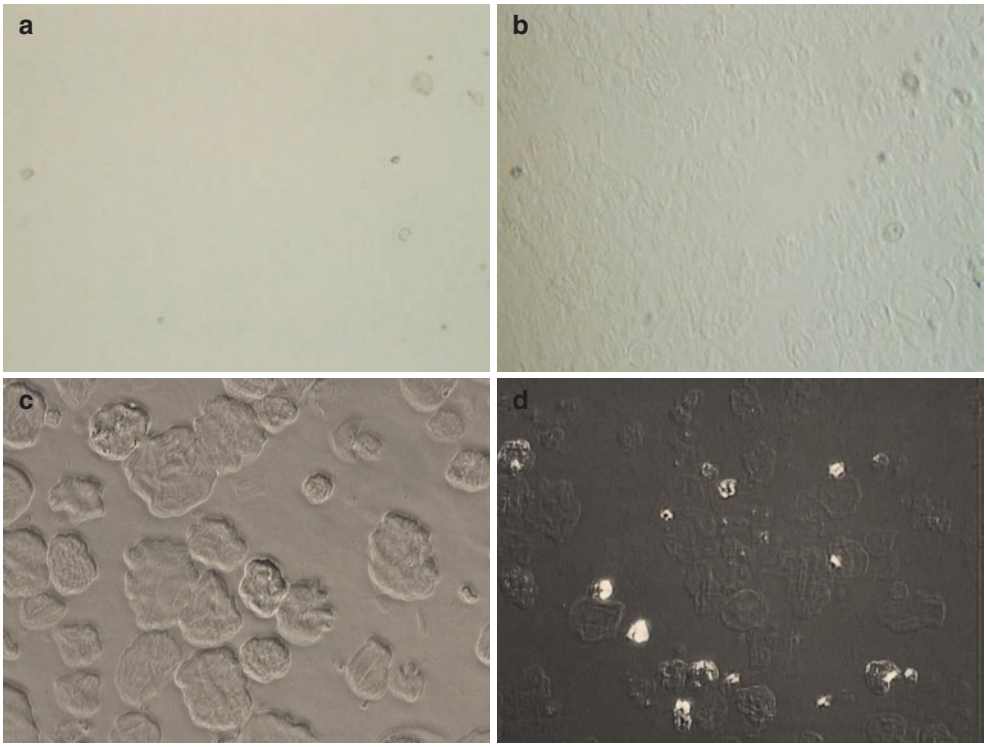

32.1 figure

Light microscopy of starch with different imaging modes. (**a**) Bright field image of cooked out starch (all or most of the crystallinity is gone). Low contrast associated with this type of sample makes it nearly impossible to see structure. (**b**) Oblique lighting. (**c**) Phase contrast. (**d**) Cross polarized image of *partially* cooked out starch. Bright granules are not cooked out and are retaining their crystallinity, or at least a portion of it

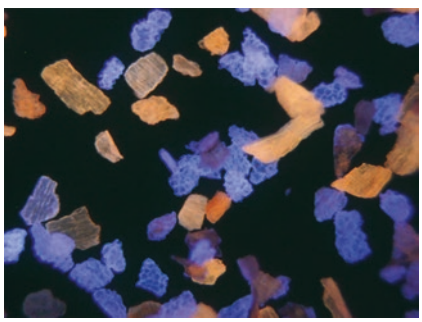

32.2 figure

Particles of wheat fiber demonstrating various colors of auto-fluorescence

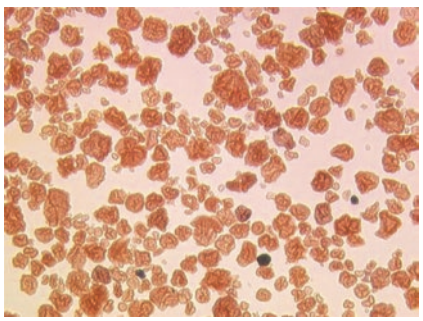

32.3 figure

Partially cooked out waxy cornstarch, stained with iodine. *Red* color is due to the amylopectin content of the starch. A few *dark*, common cornstarch granules are also seen in this image, which stain *blue* rather than *red* because they contain amylose rather than amylopectin. Iodine, being a metachromatic stain, can stain these various types of starch different colors, which aids in starch identification

species, as opposed to amylose in the common species. Iodine is referred to as a **metachromatic stain**, meaning one stain can stain different things different colors. Other specialty stains, called **polychromatic stains**, are combinations of stains that do not react with each other but will stain differing food ingredients different colors.

32.2.3 Electron Microscopy

Electron microscopy (EM), which uses electrons as the imaging agent, is of two common types: **scanning electron microscopy** (SEM) and **transmission electron microscopy** (TEM). SEM finds more frequent applications in the food industry, as described further below. Although TEM may provide an order of magnitude of higher resolution, it is not commonly used in food research mainly because it is very time consuming and requires delicate sample preparation

(e.g., extremely thin sections of the sample material, typically 60–80 nm).

The five main ways EMs differ from LMs are: (1) the imaging agent (photon vs. electron); (2) their resolving power (electrons have up to 100000 times shorter wavelength than photons, capable of resolving individual atoms); (3) their magnifying power (wide range from 20× to 1000000×); (4) LMs can provide images with visible colors to the eyes, while EMs do not give contrast in color, although false colors can be applied to SEM images to differentiate brightness levels; and (5) EMs work in high vacuum, while LMs tend to work in ambient conditions.

SEMs employ an electron beam to scan across the surface of interest. After interacting with the materials, electrons come out in several different forms. The **secondary electrons** are produced by inelastic collisions of the probe electrons (**primary electrons**) with sample electrons. Sample electrons are ejected at slower speeds than probe electrons, and with lower energy levels. They are collected at the detector for quality imaging with good depth perception. This is the primary imaging mode of SEMs. **Backscattered electrons** (BSE) involve imaging with a high-energy probe electron interacting with the sample elastically. They arrive at the detector with nearly the same speed and energy as they had in the electron probe, resulting in an image that is material dependent. Dense materials, like metals, appear bright in the BSE-SEM image, while less dense materials appear darker (e.g., carbon-based biologicals). BSE imaging is proven to be more valuable than secondary electron imaging because of the details it can provide and because it is less subject to specimen charging (Fig. 32.4).

During SEM imaging, electrons accumulate on the surface (**surface charging**), especially where it is low in conductivity. Applying a thin metal or conductive coating to the specimen surface has been an essential sample preparation step. However, low vacuum and **environmental SEM** (E-SEM) modes use water vapor or other gases within the specimen chamber to help diminish sample charging artifacts. Water vapor can, under the right conditions, also help preserve tender biological samples (including many foods and food ingredients) within the otherwise very high vacuum condition of an SEM.

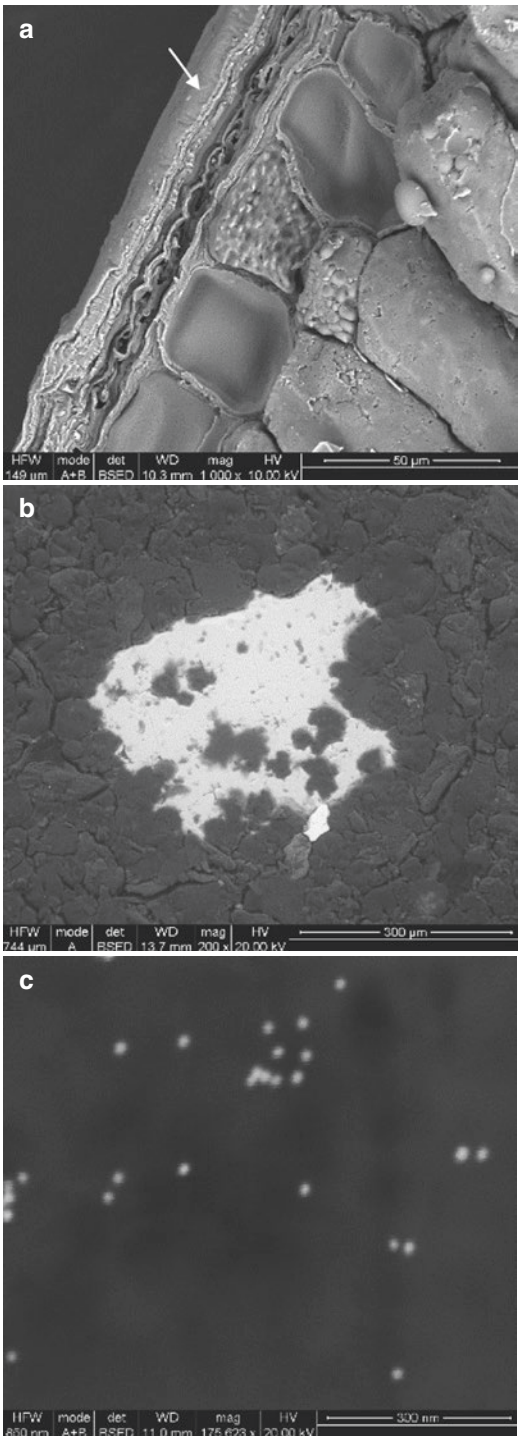

32.4 figure

BSE-SEM imaging of various materials. (**a**) A fracture through a seed in cross section. The seed coat is evident at *arrow*. Cellular structure dominates the tissue below the seed coat 1000×. (**b**) A contaminating particle (*white*) within a pharmaceutical product 200×. (**c**) 20 nm gold particles (*white dots*) used to label and identify molecular structure within a biological system 175000×

32.2.4 Energy Dispersive X-Ray Spectroscopy

When scanning electrons of SEM interact with the atoms of the specimen, it may cause electrons to migrate in between electron shells, from which an x-ray emission could be induced. The energies of the x-ray are characteristic to the atomic structures, allowing identification of the elements through an energy-dispersive spectrometer, hence the name of this

technique [**energy-dispersive spectroscopy** (EDS)]. The peaks from the EDS spectrum (x-ray energy in KeV in the X-axis and total x-ray counts in the Y-axis) represent specific elements from a periodic table (Fig. 32.5a). Additionally, both qualitative and quantitative analyses are possible for whatever elements exist within the sample.

In contrast to EDS is another technique known as **wavelength dispersive x-ray spectroscopy** (WDS), in which x-rays are diffracted to allow analysis at a certain wavelength. WDS has traditionally been better when one analyzes for a specific element with high frequency and when one needs to know the exact concentration of that one element.

Since the SEM works in a scanning fashion, restoring its electron probe in a predictable and reproducible way, we can choose specific elements from the spectrum and record a 2-D array of element dots, from which an elemental map can be generated to show distribution of compositions (Fig. 32.5b). From EDS maps, we can know not only what elements are present but how much of that element is present and precisely where that element is in the sample.

32.2.5 Atomic Force Microscopy

Atomic force microscopy (AFM), invented in 1986 [9], has found applications in most scientific disciplines, including food science [10]. The basic principle of AFM is depicted in Fig. 32.6. A very sharp tip is attached to the end of a soft **cantilever**. The tip is brought into contact to the sample, and a piezoelectric **scanner** moves the cantilever to raster scan across the surface. The cantilever deflects (up or down) as the surface topography or tip-surface interaction changes. A **laser beam** bounced off the back of the cantilever moves up and down (or left and right if there is lateral deformation of the cantilever) on a **position-sensitive photodiode detector** (PSPD) with the cantilever deflection. The photoelectric signal is then recorded and transferred into a colored map with contrast corresponding to the cantilever deflection or surface height change. Very often, to avoid large forces from the cantilever/tip damaging the scanned surface, a constant force mode is enabled in which a **feedback** signal is sent to the piezo scanner to compensate for the height change of the sample, thus maintaining a constant tip-to-sample interaction. Depending on the sharpness of the tip (**radius of curvature**) and the **spring constant** of the cantilever (usually in the range of 0.1 to a few nN/nm), the resolution of the acquired image can be in the sub-0.1 nm range, which is sufficient to resolve atoms on a surface.

Although proving to have similar minimum resolution to electron microscopy, AFM finds many advantages over EM and other microscopy techniques. First, AFM measures the true height from the sample surface, which is needed to generate a 3-D surface profile. Second, AFM is not limited by the environment it operates in. Conditions such as vacuum, ambient air, different humidity, elevated or depressed temperature, and even in liquid medium all work well for

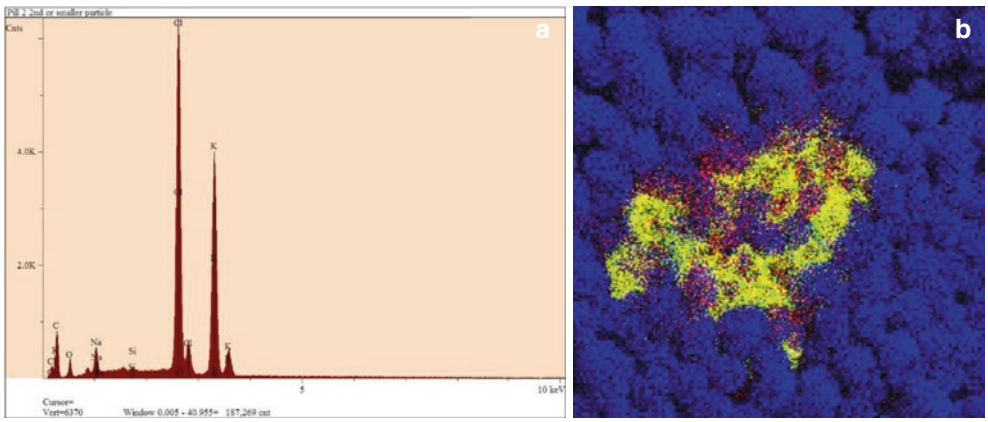

32.5 figure

EDS spectrum and EDS mapping. (**a**) An EDS elemental spectrum, with the various peaks labeled for the elements they represent. (**b**) An x-ray dot map (or x-ray-based elemental image) of an organic powder displaying a contaminating material. *Blue* represents where carbon is found in the sample. Powder particles are detected in approximate shape within the *blue* field. The contamination is seen as *yellow* (represents the element sulfur) and *red* (represents the element chlorine). *Black* represents x-ray shadowing (meaning none of those x-ray are making it to the detector)

AFM. Especially in liquid media, many biological macromolecules and living organism studies are possible [11]. Third, because the tip physically touches the sample, a variety of interactions and microscale forces can be measured [12].

Imagine when a tip is brought close to the surface, forces between the tip and surface constantly change as the tip gets closer (repulsive, long range electrostatic, etc.), touches the surface (capillary, van der Waals attraction, etc.), indents into the surface (various nanomechanical, etc.), and breaks away from the surface (adhesive, etc.). As the tip scans laterally, frictional forces also can be detected by quantifying the torsion of the cantilever.

AFM was first introduced to the food science field in 1993 with research work focusing on monitoring food protein changes. Since then, AFM applications have expanded to many areas of food science and technology, such as qualitative imaging of polysaccharides and proteins to understand their conformation and organization in certain environments, quantitative structure analysis on complex food systems (e.g., mechanical strength of food gels) to correlate with functionality, probing molecular interactions (e.g., interaction between protein and surfactant as co-emulsifiers), and molecular manipulations to observe the reactions among food macromolecules [13].

32.3 CHEMICAL IMAGING

32.3.1 Introduction

Chemical imaging is a set of analytical techniques that can generate a contrast-based image to show the distribution of the chemical or molecular composition of an object (surface or bulk). Chemical images are usually created from a **data cube** as shown in Fig. 32.7. A full spectrum (e.g., from FTIR or Raman) containing chemical signatures of all components, at a single point, is acquired. Then, either the sample is moved through a motorized mechanical or piezoelectric stage or the probing beam [e.g., focused **infrared** (IR) light for **Fourier transform infrared** (FTIR), visible laser for Raman, or electrons for SEM] scans to the next point of interest, at which a second spectrum is collected. Many points are collected on one line, and many lines of data are acquired in a raster scanning fashion. After a 2-D array of spectra is saved, various data processing mechanisms are applied to each individual

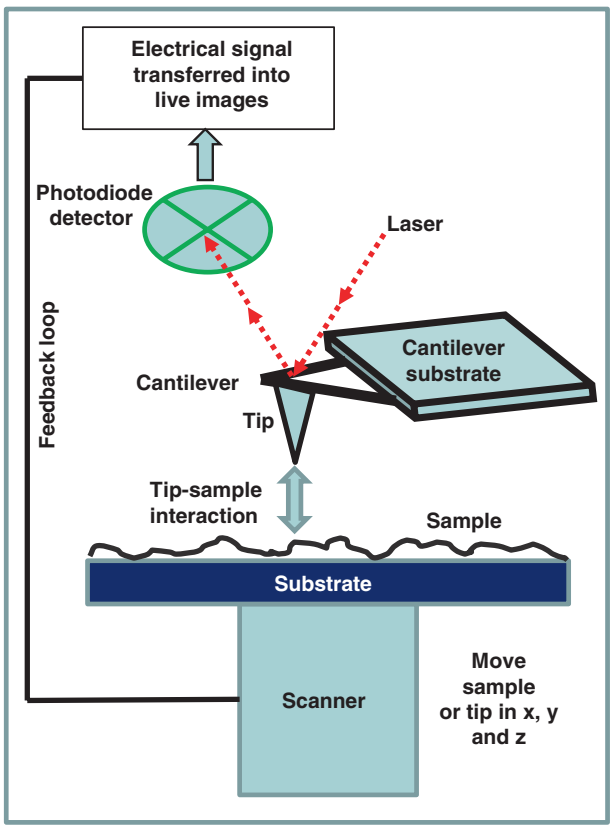

32.6 figure Schematic of a typical AFM instrument

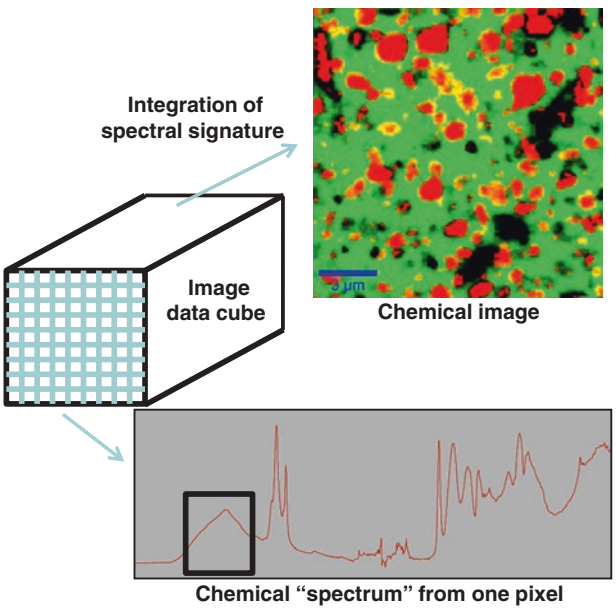

32.7 figure Schematic of chemical imaging

spectrum. Figure 32.7 shows a typical Raman spectrum, with all peaks corresponding to different functional groups, at certain vibrational modes. The peak inside the blue box is the OH stretching vibration from water in this case, and its area corresponds to the concentration of water at the current measurement location. The colored image is created by integrating this peak, for all collected spectra, with the contrast level proportional to the integrated peak area. If other components are of interest, integration of the corresponding functional peaks from the spectra can be easily applied to generate as many chemical images as possible [14].

32.3.2 Fourier Transform Infrared Microscopy

Chemical imaging with FTIR microscopy employs IR light (mid- or near-infrared) as the incident radiation. Because of the potential absorption of IR by optical components along the beam path, no transmission type of lenses is used in FTIR microscopy (like a regular light microscope, as described in Sect. 32.2.2). Spherical or parabolic mirrors are used to focus the light, and the same optical resolution limits apply as described in Eq. 32.1. Therefore, if imaging in mid-IR (2.5–50 μm), FTIR microscopy can provide chemical maps with theoretical spatial resolution of less than 1.5 μm. However, in practical application, the resolution limit of FTIR microscopy is close to 5–10 μm when selecting functional peaks with different wavelength from the spectra.

Most FTIR microscopes adopt a point-to-point scan design, meaning the detector records only one spectrum at a time when the sample is being raster scanned. A full chemical map (e.g., 100 × 100 spectra) could take 30 min – 2 h (or longer depending on the spectral resolution and pixel settings), including the time of scanning and data recording. In 1995, the introduction of the **focal plane array detector** (FPA) to the FTIR microscope brought IR imaging to a whole new level [15]. A FPA detector contains a 2-D array of **photo-sensitive elements** (e.g., mercury cadmium telluride, MCT) with each capable of capturing a complete but totally separate IR spectrum. The detector array can be anywhere from 16 × 16 to 128 × 128 elements, enabling chemical image acquisition of up to 16,384 pixels. The Digilab Stingray FPA system had the best theoretical spatial resolution of 5.5 μm using a 36× objective. Because all spectra are collected simultaneously, the time it takes to complete a whole chemical map equals the acquisition of one single spectrum, which can be from a few seconds to a few minutes, dramatically faster than traditional IR imaging.

FTIR microscopy has been widely applied in food science and technology [14]. For example, Fig. 32.8 shows a study on moisture migration through a model sugar film, mimicking a cereal coating [16].

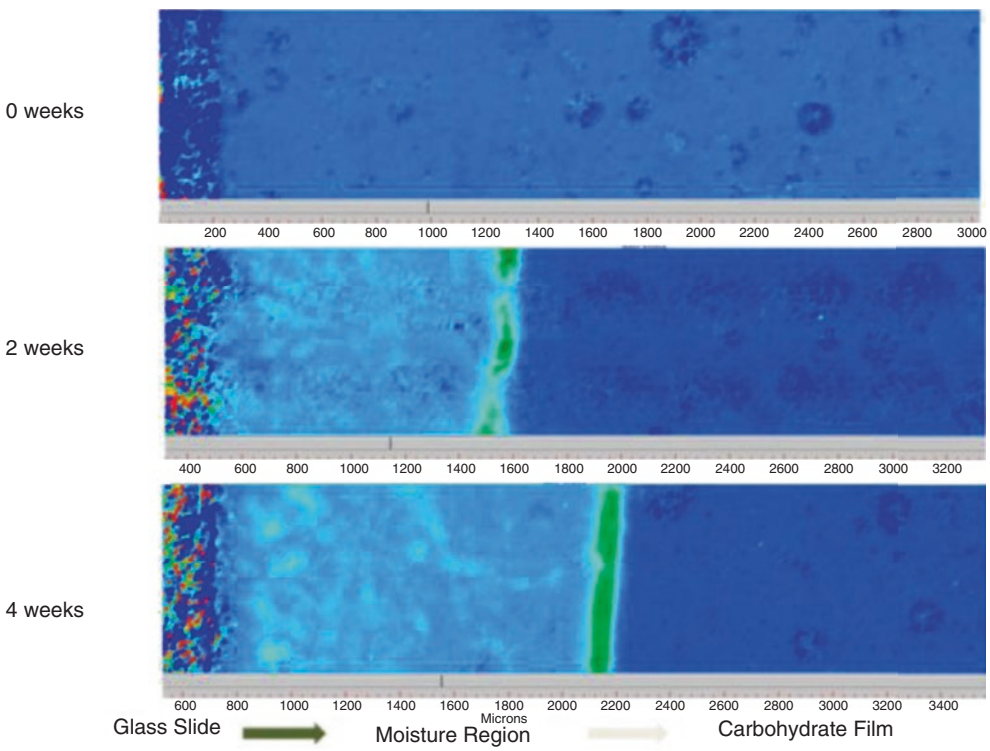

32.8 figure FT-NIR mapping of moisture sorption in a model sugar film

32.3.3 Confocal Raman Microscopy

As introduced in Chap. 8 (Sect. 8.5), Raman scattering is intrinsically weak. For Raman microscopy, because the available radiation is focused into a much smaller area, to avoid thermal damage in the sample from the laser, the effective Raman scattering is even weaker, making Raman microscopy a much less appealing technique. A great leap was seen recently in Raman microscopy technology with the development of ultra-high throughput spectrometers and high quantum efficiency **charge coupled devices** (CCDs) detectors. A high-resolution Raman image (e.g., a 200×200 pixel scan or a 40000 spectral collection) could be acquired within a few minutes or even faster, comparing to a few hours with the old generation Raman microscope [17].

As described in Chap. 8, Raman scattering is independent of excitation wavelength, meaning visible lasers can be employed for Raman experiments, which makes the design of a Raman microscope much easier than FTIR. A regular light microscope can be readily equipped with introducing an incident laser and a mechanism to collect back scattering to enable Raman measurement.

Because visible light (much shorter wavelength than IR) can be used for Raman microscopy, image resolution can be much higher than FTIR imaging. With a green laser (e.g., 532 nm) and an oil immersion objective (e.g., $NA = 1.3$), the resolution limit of a Raman image can be in the 200–300 nm range.

Confocal Raman microscopy has been used extensively in food research [18–20]. However, as described in Chap. 8, fluorescence is often troublesome in image acquisition, especially in food systems with natural ingredients. Using a longer wavelength laser (e.g., 785 nm), defocusing of the incident beam, and applying pre-imaging bleaching are common ways to reduce fluorescence, but image resolution may be deteriorated.

32.3.4 Confocal Laser Scanning Microscopy

Confocal laser scanning microscopy (CLSM) is one of the four types of **confocal microscopy** techniques (the other three are spinning-disk, micro-lens enhanced, and programmable array microscopes), which provide high-resolution chemical images based on fluorescence emission from the sample.

Figure 32.9 shows a typical setup of a confocal microscope. The incident light (a laser or white light source) enters the microscope objective through a dichroic mirror and is focused on the sample through the objective lens. The reflected or backscattered light goes back through the lens and converges at the detector surface, through which the radiation signal is recorded. With a confocal setup, a light blocking plate with a small pinhole is placed right in front of the detector at the converging point to still allow the back-focused light to reach the detector. Imaging light also may be reflected back from locations below (e.g., green lines) or above the focal plane, but it will converge before or after the pinhole, which will be blocked by the pinhole plate and is not able to reach the detector.

With this configuration, only light coming from the focal plane can be recorded by the detector. No background radiation from below or above the focal plane reaches the detector, which gives the recorded images a much sharper appearance. However, one limitation of the confocal setup is that the field of view is significantly smaller due to the size of the pinhole. Therefore, a scanning mechanism, typically through a set of vibrating mirrors, is often incorporated to provide images with a large field of view. The mirrors vibrate through piezoelectric elements, capable of providing scanning speed of 1800 Hz (lines/s) or faster. The entire focusing system (anything above the sample) is usually capable of moving in the vertical direction, allowing image acquisition at different focal planes. A 3-D image then can be generated by stacking images acquired from many focal planes.

The contrast of CLSM images is based on the fluorescence intensity from the laser's illuminating point. As described in Sect. 32.2.5, there are many ways to label the target object to give fluorescence emission. Samples are often labeled with multiple fluorophores to allow co-localization studies of a complex system.

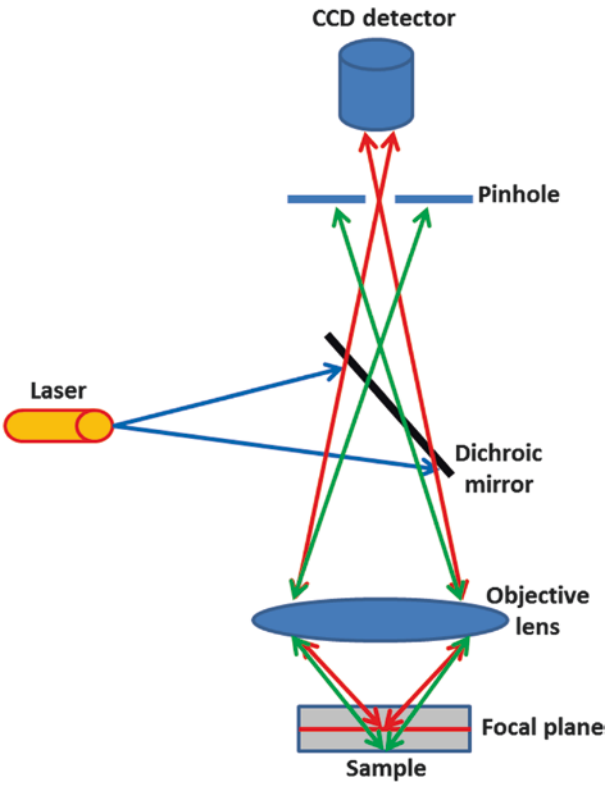

32.9 figure Schematic of a confocal microscope

CLSM has wide applications in biological and medical science disciplines but also finds popular applications in foods (e.g., imaging fat crystal structures, dairy products, food emulsions, food gels, plant materials, etc. [21]).

32.4 X-RAY DIFFRACTION

Molecules, atoms, or particles arrange differently in a solid material. When they pack in an ordered fashion, with symmetrical and repetitive pattern, the solid is called a **crystal**. Crystalline materials are rigid, have fixed melting point, can be cleaved along a definite plane, and have anisotropic physical properties such as electrical conductivity, refractive index, and thermal expansion. In contrast, **amorphous** materials have short range, or no order of molecular alignment. They are less rigid, usually do not have sharp melting points, and have isotropic physical properties.

Within a three-dimensional crystalline structure, a volume element that repeats its geometry and orientation in all directions can usually be identified as a **unit cell**, with the smallest volume often considered as the representative unit (Fig. 32.10a). The unit cell can be defined with six parameters, with three being the edge length (e.g., Fig. 32.10b) and three being the angles in between the edges (denoted as α, β, and γ, not shown). For a given crystal, when these six parameters are measured, the unit cell, or the crystal structure can be elucidated [22].

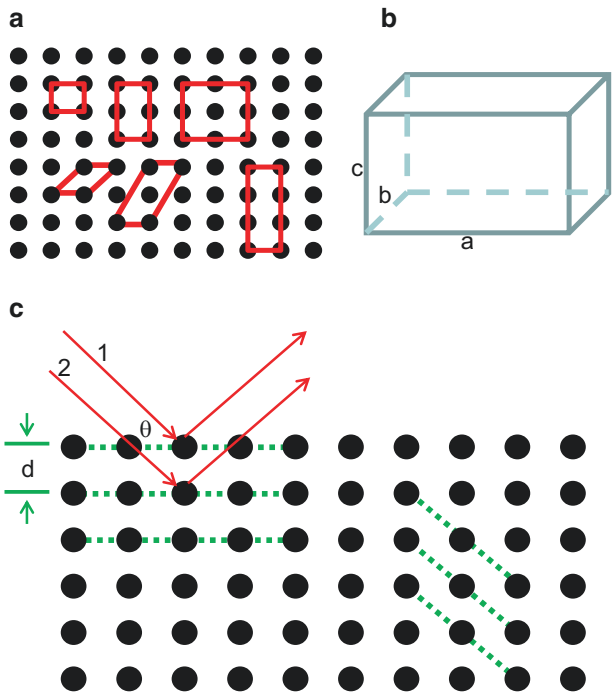

32.10 figure

Crystal unit cell and x-ray diffraction. (**a**) Repeating volume elements, or unit cells in a crystal, (**b**) Unit cell dimension parameters, (**c**) Parallel planes intersecting a unit cell, and reflection of x-rays off the planes

The structural elements (molecules, atoms, or particles) in a unit cell form parallel planes (dotted lines in Fig. 32.10c) which intersect the unit cell in many different ways. When electromagnetic radiation such as x-rays strikes the crystals, they are reflected by these planes. Assuming the incident x-ray has parallel beams (e.g., Fig. 32.10c, beam 1 and 2), to have a constructive interference between the beams reflecting off of the crystal planes, the additional distance that beam 2 travels ($2 \times d \times \sin\theta$, where d is the spacing of crystal planes and θ is the incident angle of incoming radiation) has to equal $n \times \lambda$ (n is an integer and λ is the wavelength of the radiation):

$$n\lambda = 2d \sin\theta \tag{32.2}$$

Equation 32.2 is called **Bragg's equation**. Under this condition, the reflected beams add up to give a diffraction pattern. Those with destructive interference are subtracted from each other, which produces much weaker radiation at the detector. With λ known from the x-ray source, and θ measured from x-ray/sample geometry, d can be obtained for a certain set of crystal planes. However, for a single crystal, within the scan range of θ, not all crystal planes can give **constructive diffraction**. A polycrystalline sample (powdered crystals) is usually used as an alternative to capture all diffraction patterns/peaks to resolve the complete crystal structure, and the technique is therefore referred as **powder x-ray diffraction**.

A simple schematic of an **x-ray diffractometer** (XRD) is depicted in Fig. 32.11a. The detector usually

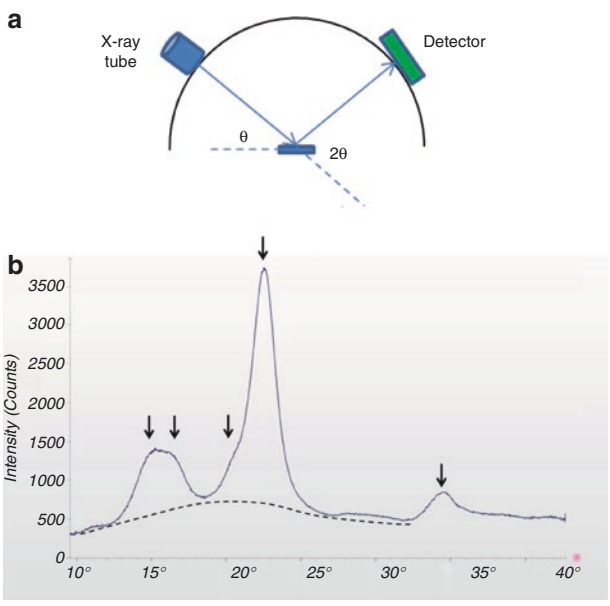

32.11 figure

Schematic of powder diffraction. (**a**) Simple schematic of an x-ray diffractometer. (**b**) XRD spectrum of crystalline cellulose. Dotted line shows the residual amorphous phase.

scans along the arc to vary 2θ, and the XRD spectrum is generated by plotting it with x-ray intensity as a function of 2θ [23].

X-ray diffraction patterns are characteristic of unit cell types and other structural properties of the crystals (e.g., lattice parameters, phase identity, crystallinity, composition, etc.). Figure 32.11b is a typical XRD spectrum for crystalline cellulose which is isolated from plant cell wall materials (from cotton linter in this case).

X-ray diffraction is a powerful tool for food research. Wide applications are found in carbohydrates (e.g., sugar, polysaccharides, etc.) and lipid/fats areas since these materials can easily form crystalline structures under application conditions [24, 25].

32.5 TOMOGRAPHY

32.5.1 Introduction

The word **tomography** is based on the two Greek words, *tomos* (meaning slice or section) and *graphe* (meaning to draw or write). The process of tomography, then, is the reconstructing of the original material, or specimen, from either a series of physical sections (through microtomy or sequential removal from the bulk) of that specimen or from a series of "optical" sections. Though tomography was originally done methodically by hand, the general practice now is to use computer assistance, hence, the term **computer-assisted tomography**. Tomography can be done using any of several possible mechanisms, such as confocal light microscopy, electron microscopy, radio frequency waves (MRI), or x-ray microscopy.

32.5.2 X-Ray Computed Tomography

X-ray computed tomography (CT) [older term is **computerized axial tomography** (CAT)] employs x-rays as the imaging agent to generate a 3-D digital image of the specimen. As the x-ray strikes through the object, a 2-D shadow image is collected on the detector, with contrast proportional to the x-ray attenuation or the physical density of the sample. The sample is rotated in single axis, and multiple images are collected with the orientation. A special computing algorithm (digital geometry processing) is applied to the series of 2-D images to construct a 3-D image that shows the inside of the specimen.

CT is both qualitative and quantitative. CT images can be rendered in both surface and volume modes. Segmentation can be applied to the images to render structures with similar density. The resolution of CT is mostly dependent on the x-ray beam size and the detector parameters. With a microscopic CT system, image resolution can be achieved in the range of a few micrometers.

CT is predominantly used in medical field but has found more and more applications in food research, e.g., to visualize fillings inside a chocolate cookie, to quantify air cell size and cell wall thickness of a gluten-free bread, to monitor bubble formation of an icing, and to study salt dissolution in a cookie dough.

32.6 CASE STUDIES

32.6.1 Fat Blends

One trend in fat-/oil-related food research is to reduce the amount of saturated fat. Saturated fat forms unique crystal structures at room temperature, which not only acts as the framework of the blends to give desired physical functionality but also provides a network to hold liquid oil. Reducing or replacing the saturated fat, but keeping the same functionality, demands a thorough understanding of the fat crystal structure. Except for ingredients, processing conditions also may be adjusted to allow manipulation of fat crystal formation.

In a fat blend case study, high oleic oil was the liquid oil fraction and palm stearin was the saturated fat fraction. The ratio of the two was varied from 90:10 to 80:20. Structuring agents, which affect crystal formation and growth, were added in small amounts, 2–4 % (e.g., monoglyceride, wax, lecithin, etc.). Functional properties such as oil-holding capacity, mechanical strength (e.g., Young's modulus), and plasticity were evaluated through different measurements. Crystallization was characterized by DSC, and crystal polymorphs were measured by XRD. Microstructure was imaged by confocal Raman microscopy and CLSM. Figure 32.12 shows some CLSM images of the fat blends with varying processing conditions and compositions. Drastic differences were observed in crystal structures (Nile red-stained liquid oil, with dark contrast corresponding to fat crystals), which correlated well with other functionality parameters.

32.6.2 Food Emulsions

To make a stable emulsion, emulsifiers with amphiphilic nature are added to prevent liquid droplets from coalescence. Common food emulsifiers are lecithin (from soy or egg yolk), mono- or diglycerides, and proteins. When concentration in a liquid is higher than its critical micelle concentration (CMC), lecithin molecules start to aggregate. The size and packing structure of the aggregates are indications of its packing ability at the oil/water interface when being used as emulsifiers. Figure 32.13 shows the microstructure characterization of emulsions prepared in a study comparing the performance of two different plant-source lecithins. TEM images show that one type of lecithin formed spherical micelles (smaller radius of curvature) and the other formed worm-like micelles. Light microscopy suggested significant differences in droplet size and morphology. CLSM shows that the emul-

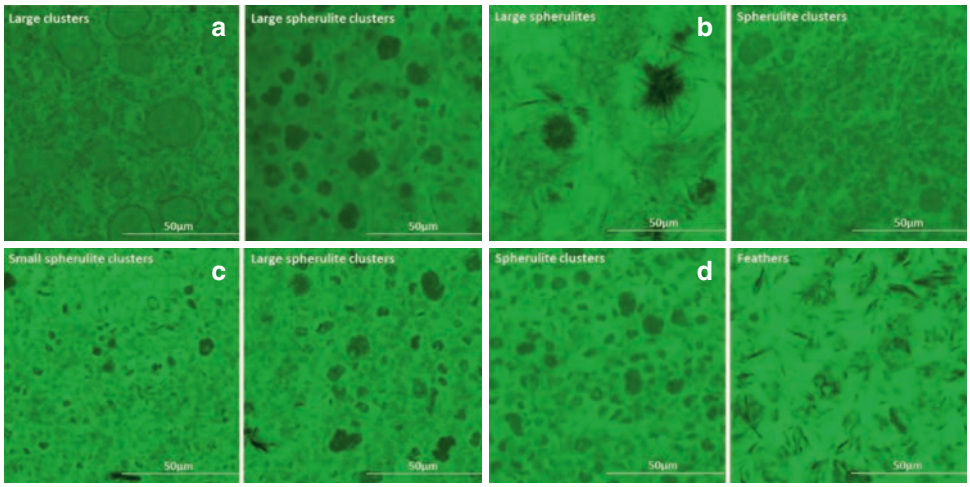

32.12 figure CLSM of fat crystal structures. (**a**) Varying cooling rate. (**b**) Different structuring agent. (**c**) Varying liquid/saturated fat ratio. (**d**) Same structuring agent but with varying concentration

sion on the left had lecithin nicely ordered at the interface of the water droplets, while the one on the right did not form the water-in-oil emulsion as desired. Lecithin stayed with the oil in the droplet instead of stabilizing at the interface. Emulsion stability measurement (through centrifuge), particle size measurement [through time-domain nuclear magnetic resonance (TD-NMR) (Chap. 10, Sect. 10.3) and particle size analyzer (Chap. 5, Sect. 5.5.2.3)], and conductivity measurement gave similar microstructure predictions.

32.7 SUMMARY

The future of food research and food production resides in controlling and manipulating food structures to give desired functionality. This chapter briefly introduced some direct and indirect microstructure characterization tools that were mostly invented or developed in and for other science disciplines. They have been borrowed by food scientists and manufacturers for many years to help better understand food systems. Some techniques have become essential tools in food science and technology. More detailed discussions of each technique can be easily found in the references cited in the text. Table 32.1 summarizes some key characteristics of these techniques.

One must be aware that none of the techniques included in Table 32.1 are universal in their applications. Foods can be very complex systems, with a very broad spectrum of types and modifications. Very often, combinations of several scientific techniques are needed to grasp the full picture of the structure of just one food type. The purpose of learning food microstructure is to be able to control and design new structures. Progress is continuously being made in this developing field, and huge opportunities are just ahead of us.

32.1 table Key characteristics of tools to examine food microstructure

Microstructure tool	*Imaging agent*	*Typical resolution*	*Key information provided*
Light microscope	Visible light	~200 nm	Morphology. Composition with histology
Fluorescence microscope	Visible light	~200 nm	Composition
SEM	Electrons	Sub-nm	Surface morphology
EDS	X-rays	Sub-nm	Elemental composition. Elemental distribution
AFM	Sharp tip	Sub-nm	Surface morphology. Interfacial forces
FTIR microscope	IR light	5–10 mm	Chemical distribution
Confocal Raman microscope	Visible laser	~200 nm	Chemical distribution
CLSM	Visible laser	~200 nm	Chemical distribution
XRD	X-rays	20–50 μm	Crystallinity
CT	X-rays	5–10 μm	3-D morphology

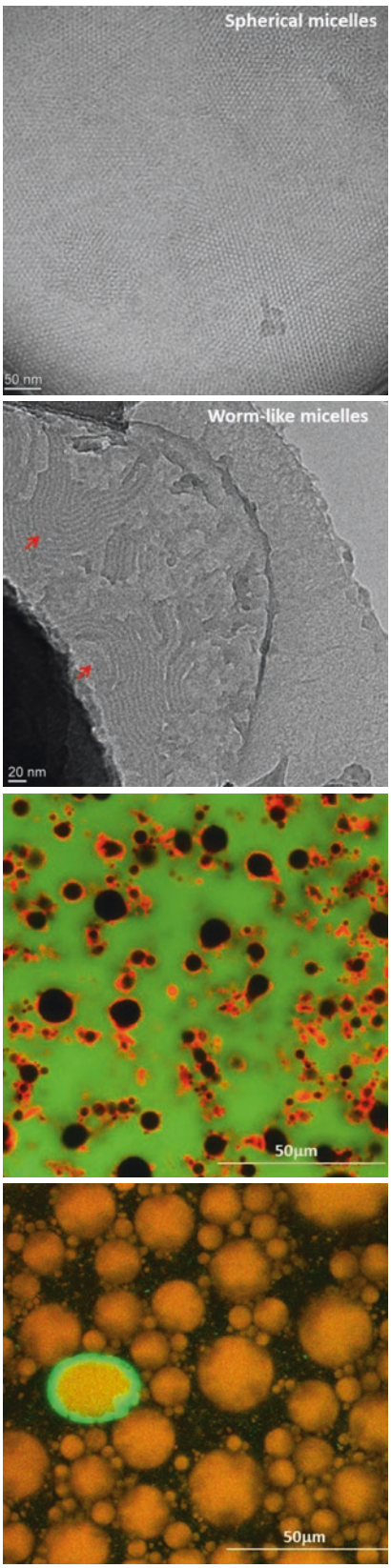

32.13 figure

Imaging characterization of emulsions with different lecithin: *Top two*-TEM; *Bottom two*-CLSM

Acronyms

2-D	Two dimensional
3-D	Three dimensional
AFM	Atomic force microscopy
CAT	Computerized axial tomography
CCD	Charge coupled device
CLSM	Confocal laser scanning microscopy
CMC	Critical micelle concentration
CT	Computed tomography
DIC	Differential interference contrast
EDS	Energy dispersive spectroscopy
EM	Electron microscopy
E-SEM	Environmental scanning electron microscopy
FPA	Focal plane array
FTIR	Fourier transform infrared
IR	Infrared
LM	Light microscopy
SEM	Scanning electron microscopy
TEM	Transmission electron microscopy
XRD	X-ray diffraction

32.8 STUDY QUESTIONS

1. What is the definition of "resolution" with regard to microscopy? How is the resolution of an optical microscope determined?
2. What is the main reason that electron microscopes can work at much higher magnifications (or resolution) than light microscopes?
3. Why do we apply a conductive coating to samples examined by an SEM? Why is a conductive coating usually not needed when examining samples using either a low vacuum SEM or an environmental SEM?
4. When using energy-dispersive x-ray spectroscopy (EDS), what carry the information telling us the elemental content of the sample, and where do they come from?
5. FT-Raman is often an option when sample has strong fluorescence. Why is it not used in Raman microscope?
6. What is "tomography" and what advantages does it have over other imaging techniques? How does computer-assisted x-ray tomography create a 3-D image?
7. You are working on a project to reduce the sugar content in gummy candies. You replaced some sugar with high-intensity sweetener and added some starch to try to maintain the elastic property. However, the candy does not look and taste like the normal gummy candy. You are asked to understand the candy's microstructure. What would be your experimental plan to do the characterization?

REFERENCES

1. Van Helden A, Dupre S, van Gent R, Zuidervaart H (eds) (2010) The origins of the telescope. KNAW Press (now Aksant Academic Publishers), Amsterdam, Netherland
2. James PJ, Thorpe N (1994) Ancient inventions. Random House Publishing, London, UK
3. Delly JG (1988) Photography through the microscope. Eastman Kodak Co., Rochester, NY
4. Green FJ (1991) The Sigma-Aldrich handbook of stains, dyes & indicators. Aldrich Chemical Co., Inc., St. Louis, MO
5. Peter G (1964) Handbook of basic microtechnique, 3rd edn. McGraw Hill, New York
6. Clark G (1981) Staining procedures. Williams & Wilkins, Essex, UK
7. Lillie RD (1977) H. J. Conn's biological stains, 9th edn. Williams & Wilkins Co., Reprinted by Sigma Chemical Co., St. Louis, MO
8. Hergert W, Wriedt T (2012) The Mie theory basics and applications (Chapter 2 authored by Wriedt T), Springer, New York
9. Binnig G, Quate CF, Gerber CH (1986) Atomic force microscope, Physical Review Letters 56:930
10. Haugstad G (2012) Atomic force microscopy: understanding basic modes and advanced applications. Wiley, New York
11. Baró AM, Reifenberger RG (2012) Atomic force microscopy in liquid: biological applications. Wiley, New York
12. Sarid D (1994) Scanning force microscopy: with applications to electric, magnetic, and atomic forces. Oxford University Press, Oxford, UK
13. Yang H., Wang Y, Lai S, An H, Li Y, Chen F (2007) Application of atomic force microscopy as a nanotechnology tool in food science. J Food Sci 72:R65
14. Sasic S, Ozaki Y (2011) Raman, infrared, and near-infrared chemical imaging. Wiley, New York
15. Lewis EN, Treado PJ, Reeder RC, Story GM, Dowrey AE, Marcott C, Levin IW (1995) Fourier transform spectroscopic imaging using an infrared focal-plane array detector, Anal Chem 67:3377
16. Nowakowski CM, Aimutis WR, Helstad S, Elmore DL, Muroski A (2015) Mapping moisture sorption through carbohydrate composite glass with Fourier transform near-infrared (FT-NIR) hyperspectral imaging. Food Biophysics 10:207
17. Dieing T, Hollricher O, Toporski J (2011) Confocal Raman microscopy. Springer, New York
18. Thygesen LG, Lokke MM, Micklander E, Engelsen SB (2003) Vibrational microspectroscopy of food. Raman vs. FT-IR. Trends Food Sci & Tech 14:50
19. Roeffaers MBJ, Zhang X, Freudiger CW, Saar BG, van Ruijver M, van Dalen G, Xiao C, Xie XS (2011) Label-free imaging of biomolecules in food products using stimulated Raman microscopy. J Biomed Optics 16(2): 021118
20. Gierlinger N, Schwanninger M (2007) The potential of Raman microscopy and Raman imaging in plant research. Spectroscopy 21:69
21. Lagali N (ed) (2013) Confocal laser microscopy: principles and applications in medicine, biology, and sciences. InTech (open access), Rijeka, Croatia
22. Yoshio W, Eiichiro M, Kozo S (2011) X-ray diffraction crystallography. Springer, New York
23. Jenkins R, Snyder R (1996) Introduction to x-ray powder diffractometry. Wiley-Interscience, New York
24. Putaux JL (2005) Morpholody and structure of crystalline polysaccharides: some recent studies. Macromolecular Symposia 229:66
25. Idziak SHJ (2012) Powder x-ray diffraction of triglycerides in the study of polymorphism, ch. 3. In: Marangoni AG (ed) Structure-function analysis of edible fats, AOCS Press, Urbana, IL